Power Electronics and Drives
3(38), No. 1, 2018 DOI: 10.2478/pead-2018-0001

Power Electronics and Drives

PMSM Servo-Drive Fed by SiC MOSFETs Based VSI

Research Article

Tomasz Tarczewski[1], Michal Skiwski[1], Lech M. Grzesiak[2], Marek Zieliński[1]

[1]*Nicolaus Copernicus University*
[2]*Warsaw University of Technology*

Received November 03, 2017; Accepted January 27, 2018

Abstract: The article presents modern PMSM servo-drive with SiC MOSFETs power devices and microprocessor with ARM Cortex core. The high switching frequency is obtained due to the application of high efficient power switching components and powerful microprocessor. It allows to achieve good dynamical properties of current control loop, proper disturbance compensation and silent operation of servo-drive. Experimental tests results obtained for two different control schemes (i.e., cascade control structure and state feedback position control) are presented.

Keywords: *PMSM • servo-drive • SiC MOSFET • FOC control • state feedback control*

1. Introduction

PMSM servo-drives are commonly used in high precision and high dynamic applications, where fast and accurate position tracking is required (Brock et al., 2017; Yang and Lin, 2016). Observed in the recent years the development of power switching components causes that it is possible to design and build vector controlled drive with high efficient SiC MOSFETs transistors. Because of this, high switching frequencies may be achieved, what would result in better dynamical properties of current control loop. By increasing the switching frequency above 20 kHz, acoustic noise may be minimized, but the time available for execution of control algorithms will decrease and these should be relatively simple. On the other hand control schemes should provide satisfactory dynamical properties of servo-drive and good compensation of load torque. The development of modern microprocessors with ARM Cortex core may be an alternative for commonly used digital signal processors (e.g., TMS320, ADSP-21061) (Skiwski et al., 2016).

Position control of PMSM servo-drive is usually realized by using cascade control structure (CCS) with PI controllers (Mandra, 2014). The main advantages of the CCS are well-known tuning rules (e.g., magnitude and symmetric optimum criterion, internal model control method) (Harnefors and Nee, 1998; Umland and Safiuddin, 1990). On the other hand, limited bandwidth of cascade controllers reported in (Preindl and Bolognani, 2013) seems to be the main drawback. Robustness against servo-drive parameter variations (e.g., moment of inertia, non-linear friction) or external load torque may be achieved by applying more complex control techniques, such as: sliding mode control, neural network based control, iterative learning control or control based on reference model (Brock, 2011; Mandra et al., 2015; Pajchrowski et al., 2006; Urbański, 2017). Good disturbance compensation and non-linearity tolerance causes, that state feedback control (SFC) may be an alternative for aforementioned control schemes (Tarczewski and Grzesiak, 2016; Tarczewski et al., 2017). Low computational complexity as well as the possibility of incorporation of internal model of reference signal (IMRS) are also advantages of SFC (Tarczewski and Grzesiak, 2009).

* *Email: ttarczewski@fizyka.umk.pl, michalskiwski@gmail.com, lech.grzesiak@ee.pw.edu.pl, marziel@fizyka.umk.pl*

The main goal of this paper is to demonstrate a prototype servo-drive with modern SiC MOSFETs power devices and with ARM Cortex core based microprocessor. This allows to apply high switching frequency what result in quiet and precise operation of PMSM servo-drive. Description of the designed and built prototype servo-drive is presented. Next, two different control schemes are implemented and experimentally verified for position tracking as well as for disturbance compensation of servo-drive.

2. Description of the prototype servo-drive

The development of SiC MOSFET power devices (Sarnowska and Rąbkowski, 2016) and microprocessors with ARM Cortex core (Skiwski et al., 2016) causes, that it is possible to design modern servo-drive with high switching frequency. In such a case, high precision, silent and efficient operation of the servo-drive should be achieved. For that reason, it was decided to design and extensively test such a device. Block diagram of a prototype drive dedicated for high switching frequency PMSM servo-drive is presented in Fig. 1.

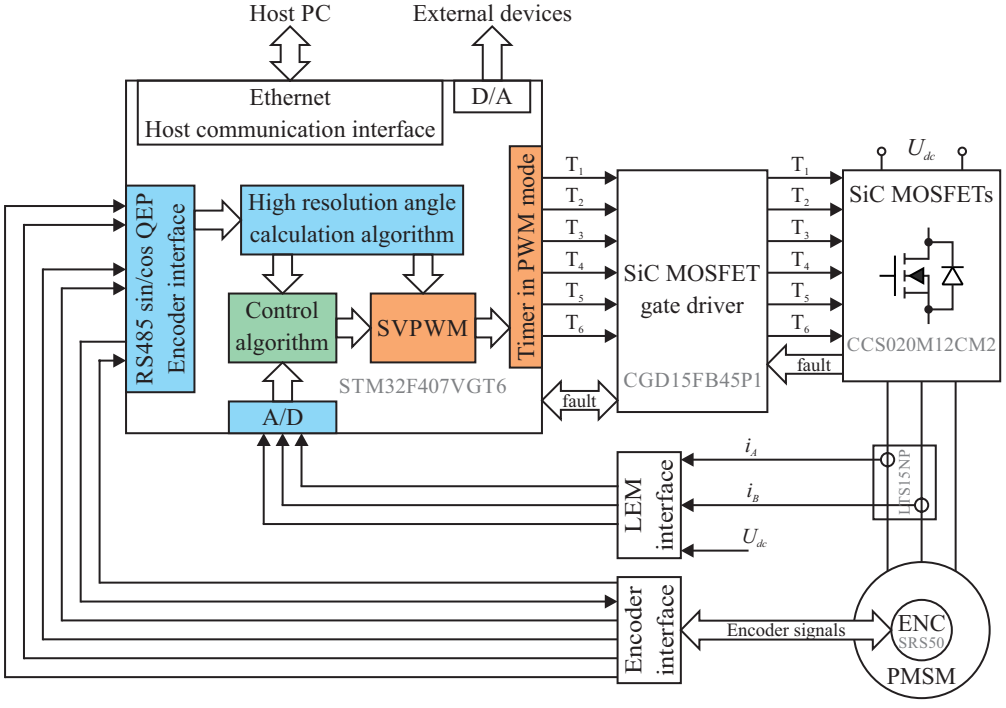

Fig. 1. Block diagram of the prototype drive with SiC MOSFETs

The prototype drive consists of: STM32F407VGT6 microcontroller from STMicroelectronics, CGD15FB45P1 six channel gate driver from Cree dedicated for SiC MOSFETs, CCS020M12CM2 2-level, 3-phase VSI with SiC MOSFETs power devices from Cree, interfaces for currents and DC-voltage measurements (LTS15NP and LV25P, respectively), single-turn absolute encoder with Hiperface interface, Ethernet interface for communication with a host PC. The angular position of the motor shaft has been obtained by using SRS50 motor feedback system from Sick. The total number of steps per revolution is equal to 32768. In order to obtain the angular velocity of the rotor shaft, the method based on fixed time (i.e., Pulse Counting) described in (Bonert, 1983) has been employed. A fixed time used for acquisition impulses from encoder was selected as a compromise between dynamical properties of angular velocity and minimization of quantization errors. Its value is equal to $32 \times T_s$. Microcontroller applied in the proposed solution is based on ARM Cortex 32-bit core that operates at 168 MHz. The device is equipped in all necessary components (i.e., fast floating point unit, PWM outputs, three 12-bit A/D converters, two 12-bit D/A converters) required in a modern drive. Moreover, Ethernet with dedicated DMA is also available, what seems to be an advantage due to the high switching frequency and, as a result, the need of sending a large amount of data between the drive and the host PC. A photo of designed and built prototype device is presented in Fig. 2.

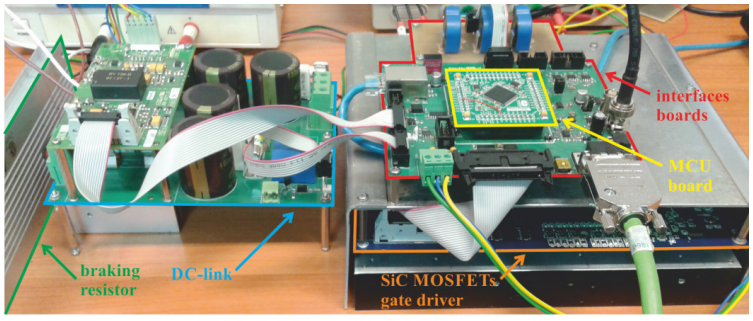

Fig. 2. Photo of the prototype VSI with SiC MOSFETs

3. Control algorithms

Designing process of control algorithms for the depicted servo-drive may be divided into two main stages. The first part covers synthesis procedure of PI controllers that are responsible for regulation of space vector current components. The second stage concerns regulation of mechanical variables (i.e., angular velocity and position) and it will be made by applying two methods: classical cascade control structure (CCS) with PI controllers and, state feedback control (SFC) approach.

3.1 Regulation of space vector current components

Synthesis procedure of PMSM current control loop requires mathematical model of the plant (i.e., motor and inverter) written in the *dq* reference frame. This is as follows

$$u_d K_p = R_s i_d + L_s \frac{di_d}{dt} - p\omega L_s i_q \tag{1}$$

$$u_q K_p = R_s i_q + L_s \frac{di_q}{dt} + p\omega\left(L_s i_d + \psi_f\right) \tag{2}$$

where: u_d, u_q – space vector components of inverter control voltages, K_p – gain of inverter, R_s, L_s – resistance and inductance of stator, i_d, i_q – space vector components of current, p – number of pole pairs, ω – angular speed, ψ_f – permanent magnet flux linkage. The aforementioned equations have been constructed with the following simplifying assumptions: dynamics and non-linearities of the inverter are omitted, *dq* inductances of the motor are equal ($L_s = L_d = L_q$). The latter assumption is valid for PMSM with surface mounted magnets while the first will be fulfilled for linear range of inverter operation and sufficiently short dead-times of power transistors (what occurs in this particular case). Since non-linear and cross-coupled terms exist in (1) and (2), the PI controllers cannot be directly designed. For that reason, linearization procedure should be applied. In this approach, a relatively simple feedback linearization method is employed (Grzesiak and Tarczewski, 2013). It requires an introduction of additional components

$$u_{nd} = p\omega L_s i_q / K_p \tag{3}$$

$$u_{nq} = -p\omega\left(L_s i_d + \psi_f\right)/K_p \tag{4}$$

into (1) and (2), respectively. As a result, linear voltage formulas have been obtained

$$u_{ld} = u_d K_p + u_{nd} K_p = R_s i_d + L_s \frac{di_d}{dt} \tag{5}$$

$$u_{lq} = u_q K_p + u_{nq} K_p = R_s i_q + L_s \frac{di_q}{dt} \tag{6}$$

These have been used during synthesis procedure of current control loop. In order to obtain coefficients of PI current controllers, an internal model control (IMC) method was applied (Harnefors and Nee, 1998). The advantage

of this method is that it requires only one parameter, the expected rise time of regulated variable (current space vector components in the considered approach), for calculation of controller coefficients. For a PI controller structure shown in Fig. 3, coefficients are calculated from the following formulas

$$K_{pi} = \alpha L_s / K_p \tag{7}$$

$$K_{ii} = R_s / L_s \tag{8}$$

where: $\alpha = \log(9)/\tau_{ri}$, τ_{ri} – the expected rise time of current. It should be noted, that coefficients of controllers were obtained for linearized model of the plant. For that reason, control signals should be supplemented by non-linear and cross-coupled components. This task has been done by introducing linearization block into current control loop. Its structure is presented in Fig. 3. From this figure it can be seen, that PI current controllers were equipped with anty-windup path in order to compensate negative impact of this phenomenon on control performance. The tracking back calculation method has been used to attenuate the integral path (Shin and Park, 2012).

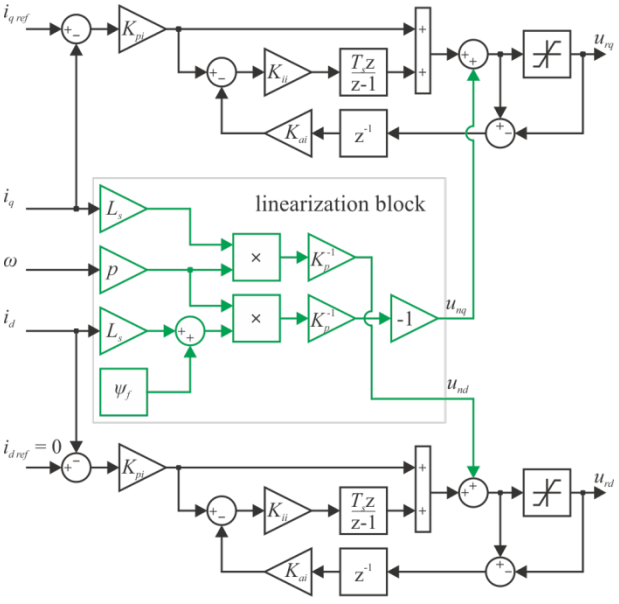

Fig. 3. Discrete current controllers with linearization block

3.2 Regulation of mechanical variables

As it was claimed before, two types of control structures (i.e., CCS and SFC) will examined for regulation of servo-drive angular velocity and position. Synthesis procedure for both of them is based on mechanical equations of the drive

$$\frac{d\omega}{dt} = \frac{1}{J}\left(K_t i_q - B\omega - T_l\right) \tag{9}$$

$$\frac{d\theta}{dt} = \omega \tag{10}$$

where: J – total moment of inertia, K_t – torque constant, B – viscous friction, T_l – load torque. It should be noted, that external load torque will be omitted during synthesis procedure but its compensation will be examined during experimental tests. It was also decided, that linear signal will be used as a reference position due to its application in servo-drives (Mandra, 2014, Tarczewski and Grzesiak, 2009). At this stage, both of control structures will operate without additional feedforward paths. During synthesis process, current control loop will be omitted due to its relatively short rise time in comparison to the dynamical behavior of mechanical variables.

Cascade control structure with discrete PI controllers responsible for regulation of angular velocity and position is shown in Fig. 4. Proposed structure has been chosen to provide zero-steady state position error for linear reference position signal and minimum transient position error observed during acceleration and deceleration of servo-drive.

As in a case of current control loop, anty-windup paths have been introduced to avoid performance deterioration of the servo-drive.

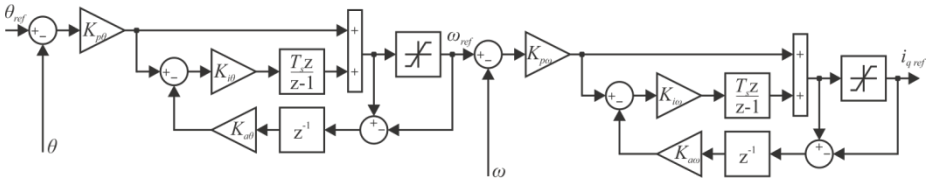

Fig. 4. Cascade control structure with discrete position and velocity controllers

An angular velocity PI controller has been tuned according to the symmetric-optimum criterion and retuned manually in order to reduce velocity overshoot and also to obtain a suitable trade-off between bandwidth and noise of velocity control loop (Tarczewski and Grzesiak, 2016; Umland and Safiuddin, 1990). Similar approach has been applied during manual selection of position controller coefficients.

In order to design state feedback position controller, mechanical equations of the servo-drive, after omitting the load torque, should be written in a state-space form. This will be augmented by internal model of reference signal (IMRS) to provide asymptotic tracking for linear reference position

$$\frac{d\mathbf{x}}{dt} = \mathbf{A}\mathbf{x} + \mathbf{B}u + \mathbf{F}r \tag{11}$$

with

$$\mathbf{x} = \begin{bmatrix} \omega \\ \theta \\ e_1 \\ e_2 \end{bmatrix}, \quad \mathbf{A} = \begin{bmatrix} -\frac{B}{J} & 0 & 0 & 0 \\ 1 & 0 & 0 & 0 \\ 0 & 1 & 0 & 0 \\ 0 & 0 & 1 & 0 \end{bmatrix}, \quad \mathbf{B} = \begin{bmatrix} \frac{K_t}{J} \\ 0 \\ 0 \\ 0 \end{bmatrix}, \quad \mathbf{F}^{\mathrm{T}} = \begin{bmatrix} 0 \\ 0 \\ -1 \\ 0 \end{bmatrix}, \quad \begin{matrix} u = i_{q\,ref} \\ r = \theta_{ref} \end{matrix} \tag{12}$$

where: e_1, e_2 – additional state-space variables necessary to assure asymptotic tracking for linear reference signal (Tarczewski and Grzesiak, 2009). The control law of resulting state feedback position controller for considered state-space model is as follows

$$u = -\mathbf{K}\mathbf{x} \tag{13}$$

where: $\mathbf{K} = [k_1\, k_2\, k_3\, k_4]$. In this approach, it was decided to obtain SFC coefficients by using pole placement method (Grzesiak and Tarczewski, 2013). Manually selected poles of considered position control system are: $p_{1/2} = -25 \pm \delta$, $p_{3/4} = -35 \pm \delta$, where $\delta = 0.05$. The latter coefficient was introduced due to the limitation of Matlab 'place' function that limits the number of the same poles to the number of control signals. As it can be seen, it was decided to use non-complex poles in order to avoid oscillations of angular position. Similar to CCS, SFC was designed to provide minimum transient position error observed during acceleration and deceleration of servo-drive, as well as zero steady-state position error for linear reference signal. Block diagram of applied SFC with anty-windup path is shown in Fig. 5.

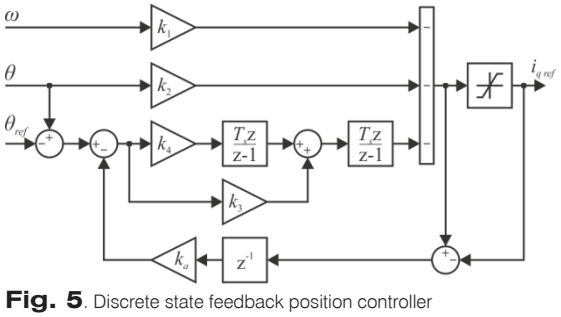

Fig. 5. Discrete state feedback position controller

4. Experimental tests

The experimental tests of designed control schemes were conducted on the laboratory stand that consists of: the main servo-drive (LTi Drives LST-127-2-30-560) equipped with single-turn absolute encoder (Sick SRS50), an auxiliary PMSM (Control Techniques) that operates in a torque mode, an additional moment of inertia and torque sensor (HBM T22/50NM). The photo of laboratory stand is shown in Fig. 6, while the main parameters of the servo-drive are summarized in Table 1.

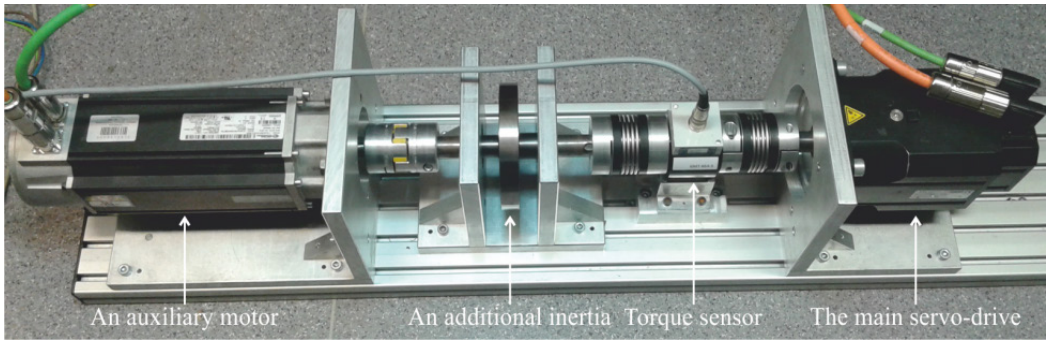

Fig. 6. Photo of laboratory stand with 1.73 kW PMSM servo-drive

Table 1. The main parameters of the servo-drive

Parameter	Symbol	Value	Unit
Rated power	P_N	1.73	kW
Rated current	I_N	5	A
Total moment of inertia	J	8.6×10^{-3}	kgm^2
Viscous friction	B	1.4×10^{-2}	Nms/rad
Stator resistance	R_s	1.05	Ω
Stator inductance	L_s	12.68	mH
Torque constant	K_t	1.14	Nm/A
Number of pole pairs	p	3	
Converter gain	K_p	100	
Switching frequency	f_{sw}	48	kHz
Sampling period	T_s	20.8(3)	μs

Proper operation of current control loop with PI controller tuned by using IMC method is shown in Fig. 7. Since high switching frequency has been employed, relatively short rise time of q-axis current was obtained ($\tau_{ri} = 0.4$ ms). This value was selected as a trade-off between dynamical properties of current control loop and measurement noise. It should assure satisfactory compensation of load torque.

For a comparative purposes, experimental response of current control loop with low switching frequency ($f_{sw} = 10$ kHz) has been recorded and the respective waveforms are shown in Fig. 8. From Fig. 8a it can be seen, that overshoot in q-axis current is observed. Moreover, lower switching frequency causes current and control voltage ripples. This proves, that by using high switching frequency a better performance of the servo-drive (e.g., faster load compensation and silent operation) may be achieved.

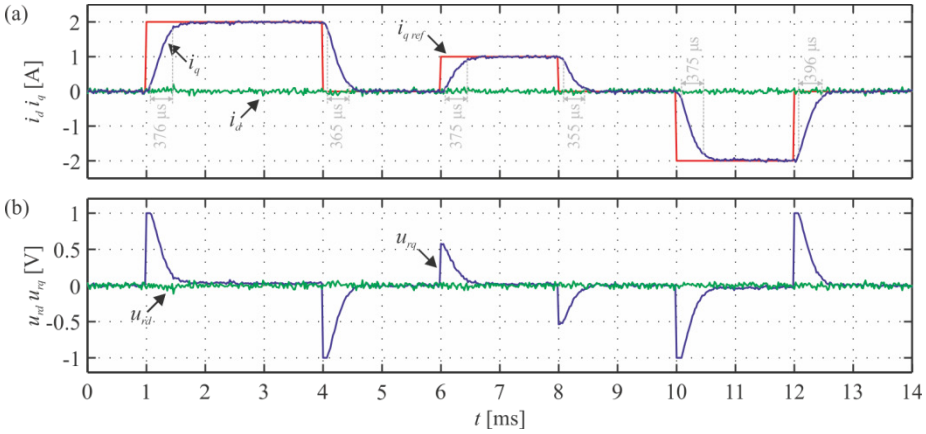

Fig. 7. Experimental response of PMSM current control loop for f_{sw} = 48 kHz and τ_{ri} = 0.4 ms: a) reference and measured *d*-*q* axis currents, b) *d*-*q* control voltages

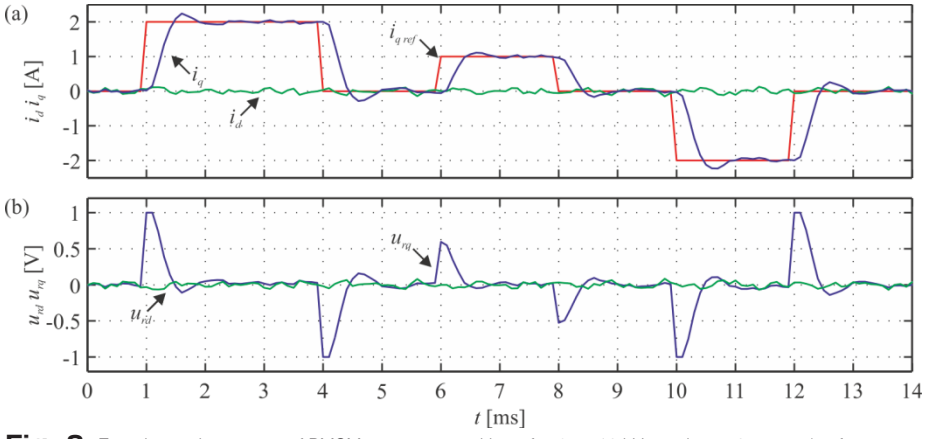

Fig. 8. Experimental response of PMSM current control loop for f_{sw} = 10 kHz and τ_{ri} = 0.4 ms: a) reference and measured *d*-*q* axis currents, b) *d*-*q* control voltages

Experimental results obtained for CCS during position tracking are presented in Fig. 9. It should be noted, that the proposed control structure assures asymptotic tracking for linear reference position. Dynamical properties of the servo-drive are limited by the boundary value of *q*-axis current. From Fig. 9.b it can be seen, that suppressed oscillations exist during position tracking for CCS. The maximal value of transient position error observed during acceleration is equal to e_θ = 1.642 rad, while the maximal value recorded during deceleration is equal to e_θ = 1.42 rad.

Experimental response of PMSM servo-drive with SFC and IMC is shown in Fig. 10. Due to the application of IMRS, asymptotic tracking for linear reference position occurs. Since non-complex poles have been used during synthesis process of SFC, position oscillations don't exist, but slightly worst tracking performance during transient is observed. The maximal value of transient position error observed during acceleration is equal to e_θ = 2.077 rad, while the maximal value recorded during deceleration is equal to e_θ = 1.894 rad. In order to improve tracking performance during transient, a feedforward path should be added, what is beyond the scope of this paper. Similar to results recorded for CCS, dynamical behavior is mainly limited by the boundary value of *q*-axis current.

The ability to load torque compensation of proposed control schemes (i.e., CCS + IMC and SFC + IMC) were also tested. An external load torque $T_l \approx 3$ Nm has been imposed to tested PMSM servo-drive for $t \in$ (100; 600) ms. As a result, an instantaneous position error is observed for both examined control structures (Fig. 11.b and Fig. 12.b) and it is properly compensated. This proves that designed control structures may be successfully applied in the designed modern servo-drive with high switching frequency.

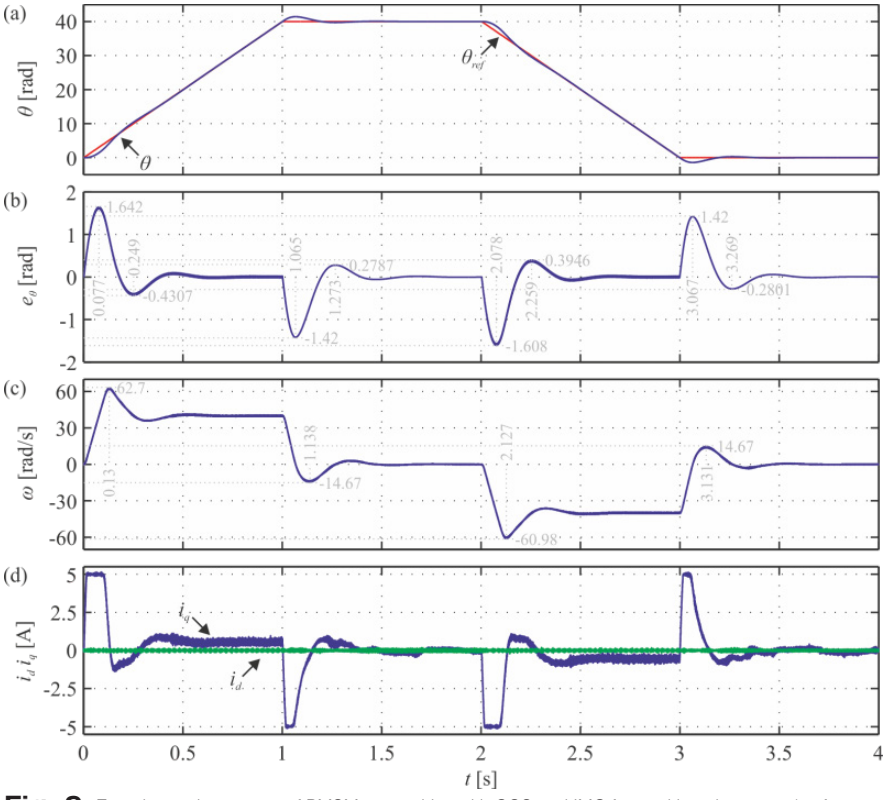

Fig. 9. Experimental response of PMSM servo-drive with CCS and IMC for position changes: a) reference and measured position, b) position error, c) angular velocity d) *d-q* axis currents

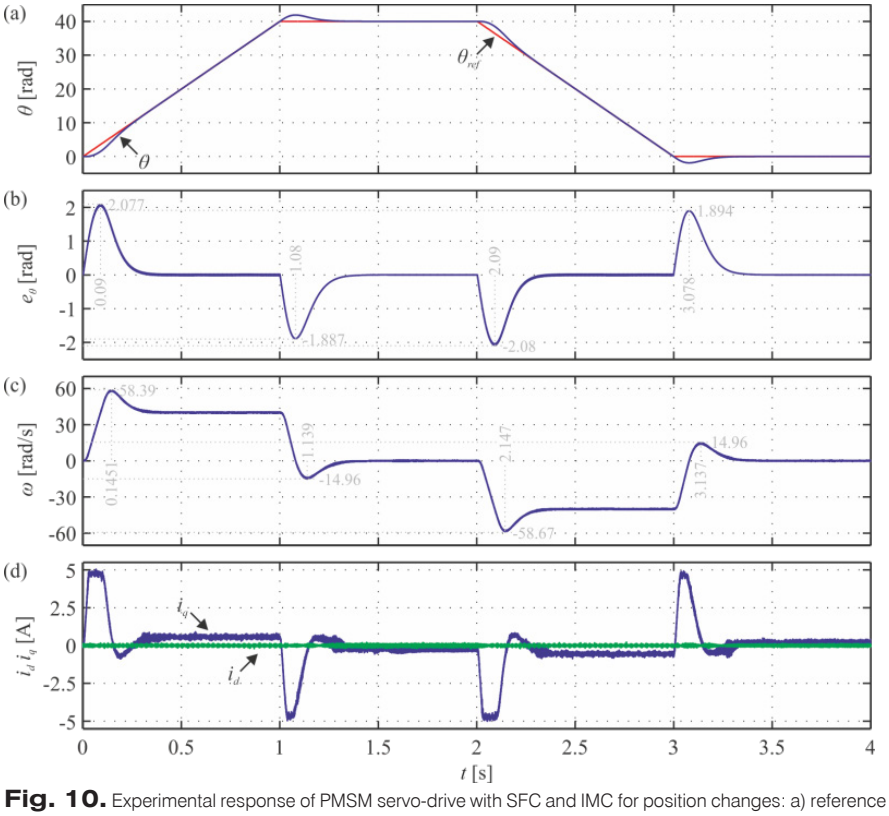

Fig. 10. Experimental response of PMSM servo-drive with SFC and IMC for position changes: a) reference and measured position, b) position error, c) angular velocity d) *d-q* axis currents

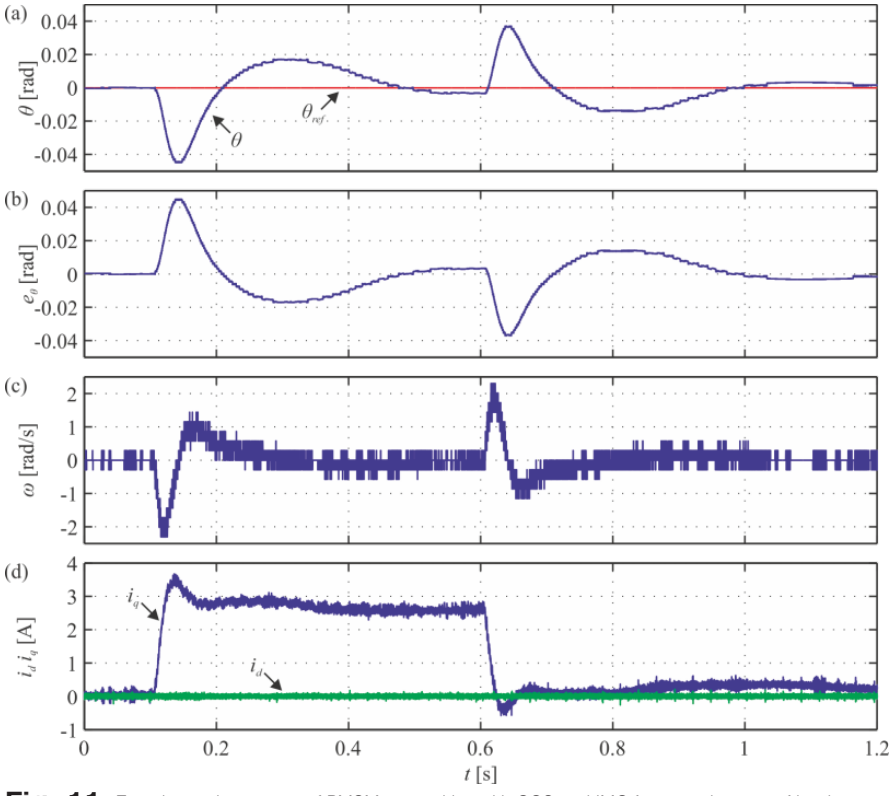

Fig. 11. Experimental response of PMSM servo-drive with CCS and IMC for step changes of load torque: a) reference and measured position, b) position error, c) angular velocity d) *d-q* axis currents

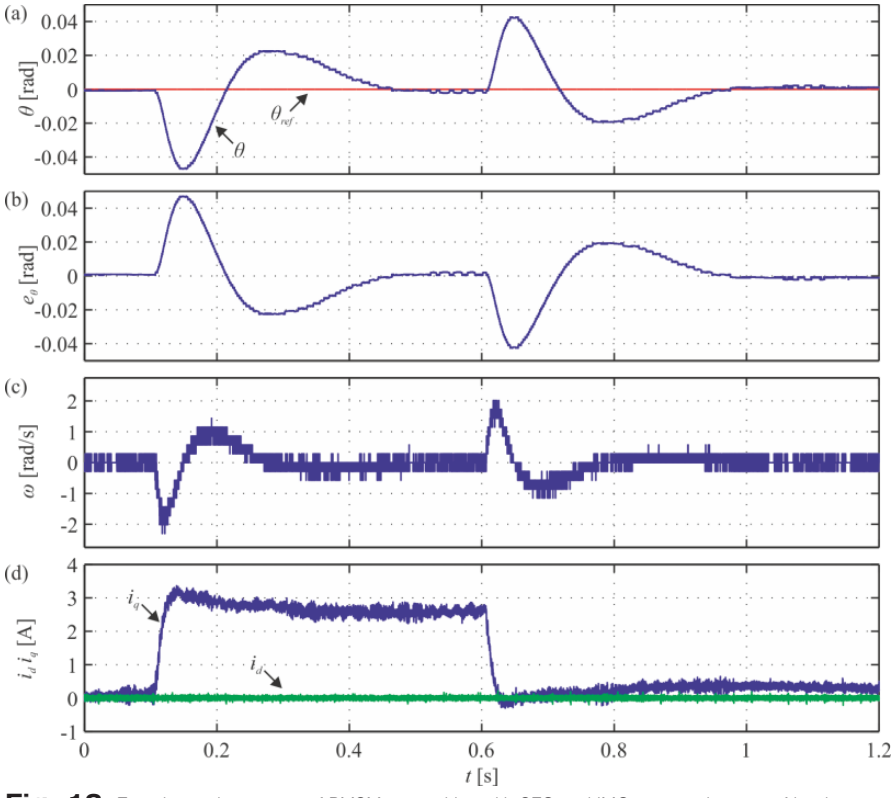

Fig. 12. Experimental response of PMSM servo-drive with SFC and IMC to step changes of load torque: a) reference and measured position, b) position error, c) angular velocity d) *d-q* axis currents

Finally, the time needed for execution of designed control algorithms was investigated and results are shown in Fig. 13. It can be seen, that time required for SFC + IMC is slightly longer in comparison to execution time of CCS + IMC. It is caused by implementation of IMRS responsible for asymptotic tracking of linear reference position. It should be noted, that total times recorded for both control schemes are shorter that half of the sampling period what guarantees proper execution of algorithms for high switching frequency (f_{sw} = 48 kHz in this particular case).

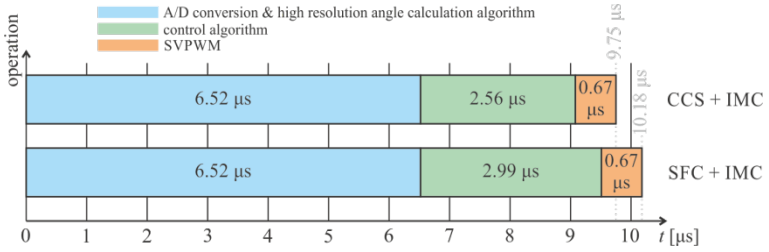

Fig. 13. Execution time of designed control algorithms

5. Conclusion

In this paper, modern PMSM servo-drive with SiC MOSFETs voltage source inverter has been presented. High switching frequency allows silent and efficient operation of servo-drive and assures good compensation of load torque. Two control schemes have been designed and implemented to provide asymptotic tracking of linear reference position. Obtained experimental results indicate the possibility of high frequency operation of both control schemes. Due to free-programming ability of the designed and built servo-drive, implementation and investigation of more complex control algorithms is planned.

References

Bonert, R. (1983). Digital Tachometer with Fast Dynamic Response Implemented by a Microprocessor. *IEEE Transactions on Industry Applications*, 19(6), pp. 1052-1056.

Brock, S. (2011). Sliding Mode Control of a Permanent Magnet Direct Drive Under Non-Linear Friction. *COMPEL*, 30(3), pp. 853-863.

Brock, S., Łuczak, D., Pajchrowski, T. and Zawirski, K. (2017). Selected methods for a robust control of direct drive with a multi-mass mechanical load. In: J. Kabziński, ed., *Advanced Control of Electrical Drives and Power Electronic Converters*. Springer, pp. 75-98.

Grzesiak, L. M. and Tarczewski, T. (2013). PMSM Servo-Drive Control System with a State Feedback and a Load Torque Feedforward Compensation. *COMPEL*, 32(1), pp. 364-382.

Harnefors, L. and Nee, H.-P. (1998). Model-Based Current Control of AC Machines Using the Internal Model Control Method. *IEEE Transactions on Industry Applications*, 34(1), pp.133-141.

Mandra S. (2014). Comparison of Automatically Tuned Cascade Control Systems of Servo-Drives for Numerically Controlled Machine Tools. *Elektronika ir Elektrotechnika*, 20(3), pp. 16-23.

Mandra, S., Gałkowski, K., Aschemann, H. and Rauh, A. (2015). Guaranteed cost iterative learning control – an application to control of permanent magnet synchronous motors. In: *IEEE 9th International Workshop on Multidimensional (ND) systems (NDS), Portugal*.

Pajchrowski, T., Urbański, K. and Zawirski, K. (2006). Artificial neural network based robust speed control of permanent magnet synchronous motors. *COMPEL*, 25(1), pp. 220-234.

Preindl, M. and Bolognani, S. (2013). Model Predictive Direct Speed Control with Finite Control Set of PMSM Drive Systems. *IEEE Transactions on Power Electronics*, 28(2), pp. 1007-1015.

Sarnowska, A. and Rąbkowski, J. (2016). Hard and soft switching operation of the half-bridge based on 900V SiC MOSFETs. In: *IEEE IECON Conference, Italy*. pp. 7167-7172.

Shin, H.-B. and Park, J.-G. (2012). Anti-Windup PID Controller with Integral State Predictor for Variable-Speed Motor Drives. *IEEE Transactions on Industrial Electronics*, 59(3), pp. 1509-1516.

Skiwski, M., Tarczewski, T. and Grzesiak, L. M. (2016). PMSM Drive Based on STM32F4 Microcontroller. *Poznan University of Technology Academic Journals. Electrical Engineering*, 87, pp. 377-387.

Tarczewski, T. and Grzesiak, L. M. (2016). Constrained State Feedback Speed Control of PMSM Based on Model Predictive Approach. *IEEE Transactions on Industrial Electronics*, 63(6), pp. 3867-3875.

Tarczewski, T. and Grzesiak, L. M. (2009). High Precision Permanent Magnet Synchronous Servo-Drive with LQR Position Controller. *Przegląd Elektrotechniczny*, 85(8), pp. 42-47.

Tarczewski, T., Skiwski, M. and Grzesiak, L. M. (2017). Constrained non-stationary state feedback speed control of PMSM. In: *EPE'17 ECCE-Europe Conference, Poland*.

Umland, J. and Safiuddin, M. (1990). Magnitude and Symmetric Optimum Criterion for the Design of Linear Control Systems: What Is It and How Does It Compare with the Others? *IEEE Transactions on Industry Applications*, 26(3), pp. 489-497.

Urbański, K. (2017). A New Sensorless Speed Control Structure for PMSM Using Reference Model. *Bulletin of the Polish Academy of Sciences Technical Sciences*, 65(4), pp. 489-496.

Yang, S. M. and Lin, K. W. (2016). Automatic Control Loop Tuning for Permanent-Magnet AC Servo Motor Drives. *IEEE Transactions on Industrial Electronics*, 63(3), pp. 1499-1506.